The Design and Manufacture of a Microfluidic Reactor for Synthesis of Cadmium Selenide Quantum Dots Using Silicon and Glass Substrates

Peter Gonsalves
Materials Engineering Department
California Polytechnic State University
Advisor: Dr. Richard Savage

June 2, 2011

Approval Page

Project Title: The Design and Manufacture of a Microfluidic Reactor for Synthesis of Cadmium Selenide Quantum Dots Using Silicon and Glass Substrates

Author: Peter Gonsalves

Date Submitted: June 2, 2011

CAL POLY STATE UNIVERSITY
Materials Engineering Department

Since this project is a result of a class assignment, it has been graded and accepted as fulfillment of the course requirements. Acceptance does not imply technical accuracy or reliability. Any use of information in this report is done at the risk of the user. These risks may include catastrophic failure of the device or infringement of patent or copyright laws. The students and staff of Cal Poly State University, San Luis Obispo cannot be held liable for any misuse of the project.

Prof. Richard Savage _____

Project Adviser Signature

Prof. Trevor Harding _____

Department Chair Signature

Acknowledgments

I would like to thank the following people for making my senior project possible.

- Boeing for project funding
- General LED for project funding
- Dr. Richard Savage (Materials Engineering) for guidance and experience

Table of Contents

Table of Figures

List of Tables

Abstract

THE DESIGN AND MANUFACTURE OF A MICROFLUIDIC REACTOR FOR SYNTHESIS OF CADMIUM SELENIDE QUANTUM DOTS USING SILICON AND GLASS SUBSTRATES

By Peter Robert Gonsalves

A microfluidic reactor for synthesizing cadmium selenide (CdSe) quantum dots (QDs) was synthesized out of silicon and Pyrex glass. Microfabrication techniques were used to etch the channels into the silicon wafer. Holes were wet-drilled into Pyrex glass using a diamond-tip drill bit. The Pyrex wafer was aligned to the etched silicon wafer and both were anodically bonded to complete the microfluidic reactor. Conditions for anodic bonding were created by exposing the stacked substrates to 300V at ~350^{o}C under 5.46N of force. Bulk CdSe solution was mixed at room temperature and treated as a single injection. The syringe containing bulk CdSe solution was interfaced to the microfluidic reactor by using Polydimethylsiloxane (PDMS) as a ferrule. Tygoprene® and stainless-steel tubing transported the bulk CdSe solution in and the QDs out of the microfluidic reactor. The microfluidic reactor was placed on a hot plate at 225^{o}C, creating conditions for the QD chemical reaction to occur within the etched channels. The CdSe solution was injected into the channels by a syringe pump at a constant injection rate of 20mL/hr. This pump rate allowed for nucleation and growth of the QDs to occur during laminar flow through the microfluidic channels. Pressure was the most significant constraint; therefore, QD residence time was controlled by varying the length of the channels while keeping the pump rate (pressure) constant. The QD fluorescence Full-Width-Half-Max is directly proportional to their size distribution. Shorter channel lengths (2.5 cm) synthesize smaller QDs than longer lengths (12.5 cm). On a single microfluidic device, an array of various channel lengths was developed that can synthesize an array of QDs with discrete spectral profiles.

Keywords: Materials Engineering, Quantum Dot, Cadmium Selenide, Fluorescence, Microfluidics, PDMS, Anodic Bonding, Quantum Confinement

1 Introduction and Background

1.0 Problem Statement

The current process of fabricating quantum dots in the California Polytechnic State University (Cal Poly) Nanotechnology Lab is on the bulk scale (10-15mL). Synthesis on this scale produces a broad spectrum of nanoparticles, characterized by their full-width-half-maximum fluorescence spectral profile. There is a need to create a process of synthesizing quantum dots with a tighter size distribution. A microfluidic reactor can synthesize the same CdSe quantum dots under carefully controlled conditions and produce a more discrete spectral profile. My goal was to create a microfluidic reactor capable of synthesizing CdSe quantum dots by using silicon and glass substrates.

1.1 Quantum Dots Defined

Quantum dots are semiconductor crystals made up of hundreds of atoms that are typically 2-10 nm in diameter. Due to their small size, quantum dots display properties that combine classic and quantum physics. The combination of behaving like a bulk material, while preserving characteristics of individual atoms makes quantum dots unique because properties can be changed simply by altering their size [1].The size of the quantum dots can be determined from their optical properties (Figure 1).

Figure 1 - A spectrum of quantum dot emissions, with quantum dot size increasing from left to right (band gap getting smaller left to right) [2].

Understanding why and how quantum dots behave the way they do begins with the electronic structure of the atoms that make up the quantum dots.

1.1.1 Molecular Theory and Band Orbitals

All atoms are basically composed of positively charged nuclei, surrounded by a negatively charged electron cloud. The Lewis Structure approach provides a simple method for determining the electronic structure of many molecules. A more general, but slightly more complicated approach is the Molecular Orbital (MO) Theory, which builds on the electron wave functions of quantum mechanics to describe chemical bonding. MO theory suggests that electrons exist in energy levels called orbitals. The orbitals are thought of as shells that surround the nucleus. Shells that are closest to the nucleus are at a lower energy state than shells that are further away. Electrons within an atom often move to different orbitals to keep the atom in its lowest energy state.

One of the fundamental rules governing the mechanics of MO theory is that atomic orbitals are combined to create molecular orbitals; the number of molecular orbitals formed equals the number of atomic orbitals used [3]. Hydrogen, for example, is the simplest of all molecules. In its atomic form, hydrogen has only a single orbital (1s) with a single electron (Figure 2).

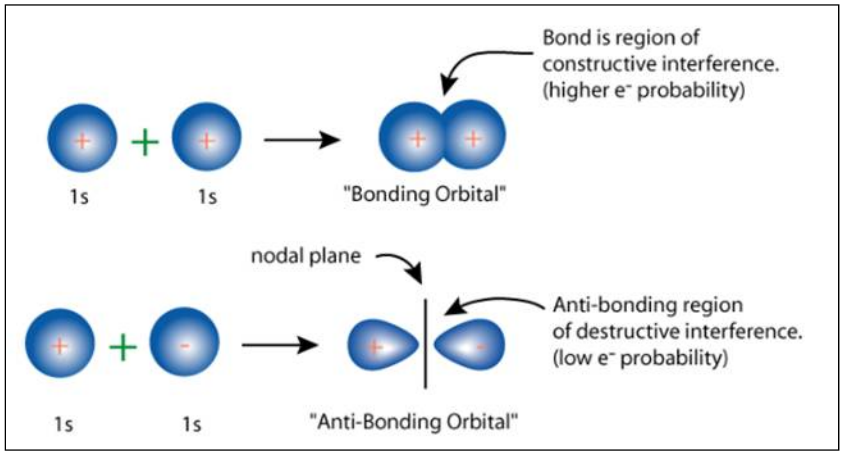

Figure 2 - The bonding of 2 hydrogen atoms is either constructive (bonding) or destructive (anti-bonding) interference [3].

The energy of an H_2 molecule with 2 electrons in the bonding orbital is less than the combined energies of the 2 separate hydrogen atoms. Conversely, the energy of the H_2 molecule with the 2 electrons in the anti-bonding orbital is higher than the combined energies of the 2 separate hydrogen atoms (Figure 3).

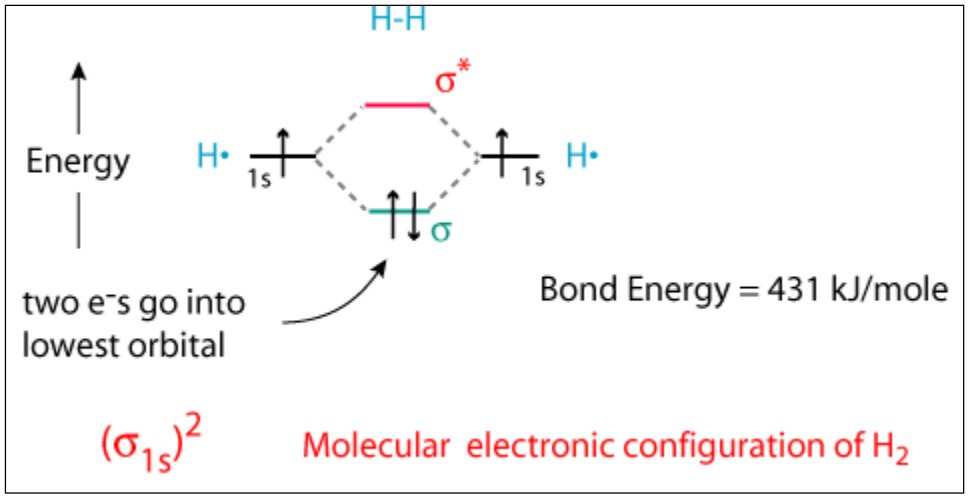

Figure 3 - Molecular orbital energy diagram. When two atomic orbitals combine to form two molecular orbitals, the orbital energies shift. The net change in energy is the same, but now there is a low energy and high energy orbital. The electrons move into the more stable, low energy, bonding orbital [3].

There is a greater probability that the 2 electrons from the original system will move to occupy the bonding orbital because it creates a lower energy state, which is preferred by nature because the molecule decreases in energy [4].

When this model is extended out to materials with more than two atoms, the number of available orbitals also increases (Figure 4), causing the orbital energies to shift. The end result is that the energy between levels are so small they can be treated as a continuous band of energies. The bonding orbital becomes the valence band, while the antibonding orbital becomes the conduction band [8].

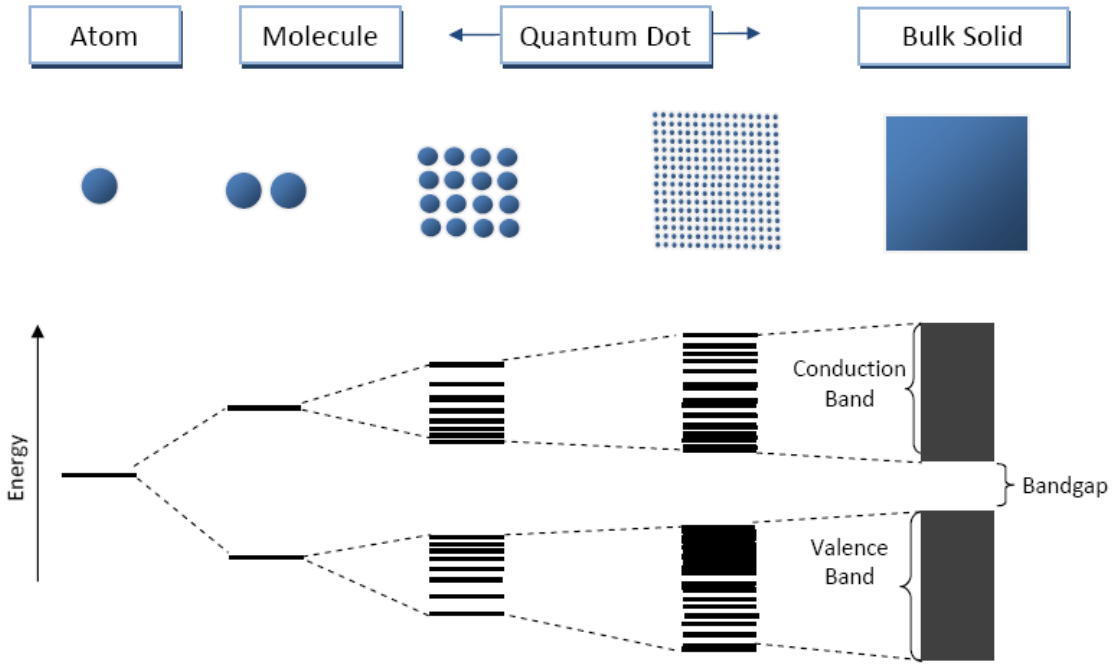

Figure 4 - Evolution of molecular orbitals into electronic energy bands. The point at which the discrete energy levels become a continuous band is where quantum dots cease being quantum and become a bulk solid.

The energy gap between the valence and conduction bands is called the bandgap [4]. Electrons are unable to occupy the bandgap region. The point where the discrete energy levels become a continuous band is the point at which a quantum dot is considered a bulk solid, approximately 10nm in size.

The only way an electron in the valence band of a natural bulk semiconductor can jump the bandgap to the conduction band is to acquire enough energy to do so. In a bulk material, this is not possible without the help of an outside stimulus, such as heat or voltage. Since quantum dots are smaller than bulk materials, an excitation source such as a high energy photon emitting light can induce electrons to jump the gap to the conduction band. The excited electron now in the conduction band and the “hole” it left

behind in the valence band are considered an exciton pair (Figure 5). The physical distance between them is called the Exciton Bohr radius [5].

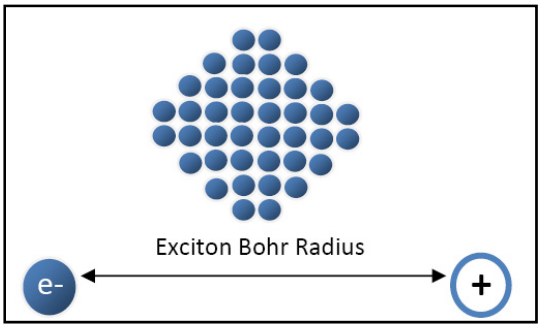

Figure 5 - The Exciton Bohr radius is the distance between an excited electron and the hole that it left behind when jumping the bandgap. The nanoparticle above is smaller than this distance so it experiences a phenomenon known as quantum confinement.

In a bulk material, the Exciton Bohr radius is much smaller than the size of the material itself, so the radius can extend to its full natural limit; however, in a quantum dot the Exciton Bohr radius is close to or larger than the material. This occurs around 10nm and the resulting exciton pairs are limited by the size of the material. Excited electrons cannot move to their full natural radius because the surface of the quantum dot is holding them back [8], which is an effect called quantum confinement (Figure 6).

1.1.2 Quantum Confinement

In bulk materials, the number of energy states available to the electrons is a virtually infinite logarithmic curve. Only as the dimensions of the material are reduced to that below the Exciton Bohr radius do we see certain energy states become unavailable. In 2D films, the excitons can extend fully in 2 directions, which are called quantum planes.

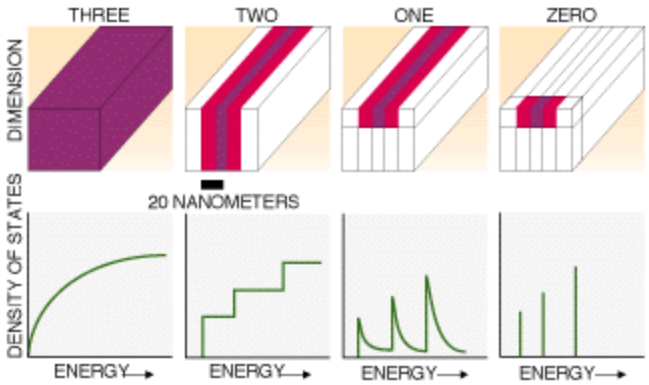

Figure 6 - Diagram showing the effects of quantum confinement for planes, wires, and dots [6].

Quantum wires further restrict the number of available energy states, limiting excitons to extend in only one direction. When the entire material is smaller than the Exciton Bohr radius in all directions only discrete energy levels remain, and only then do we truly have a quantum dot [8].

As a result of quantum confinement, adding or removing a single orbital impacts the total energy level of the system. As atoms are added, energy levels are added to the top of the valence band and the bottom of the conduction band. The result is a decrease in the total size of the bandgap; thus, creating a tunable bandgap [5].

1.1.3 Fluorescence

Fluorescence is the unique property of quantum dots that makes them so desirable. The color seen in a bulk material is the product of an excited electron jumping up to the conduction band. Immediately after jumping to the conduction band, the electron falls back down and emits a photon with energy equal to the bandgap of the material (Figure 7).

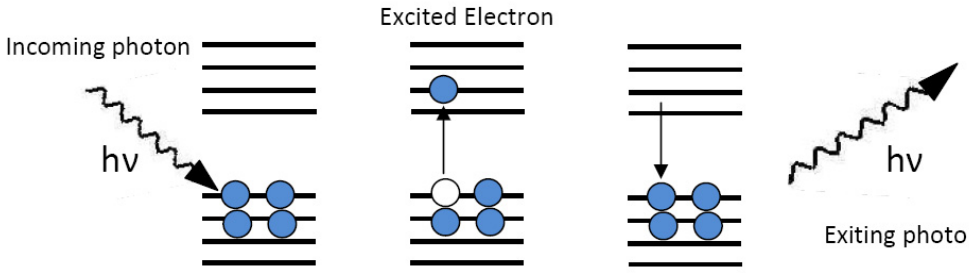

Figure 7 - Process of exciting an atom with a high energy photon and releasing a lower energy photon back out.

The same process holds true with quantum dots; however, since the bandgaps of quantum dots can be changed with an increase and decrease in size, it is possible to alter the color of the emitted photons [7]. This effect can be summarized as follows (Figure 8):

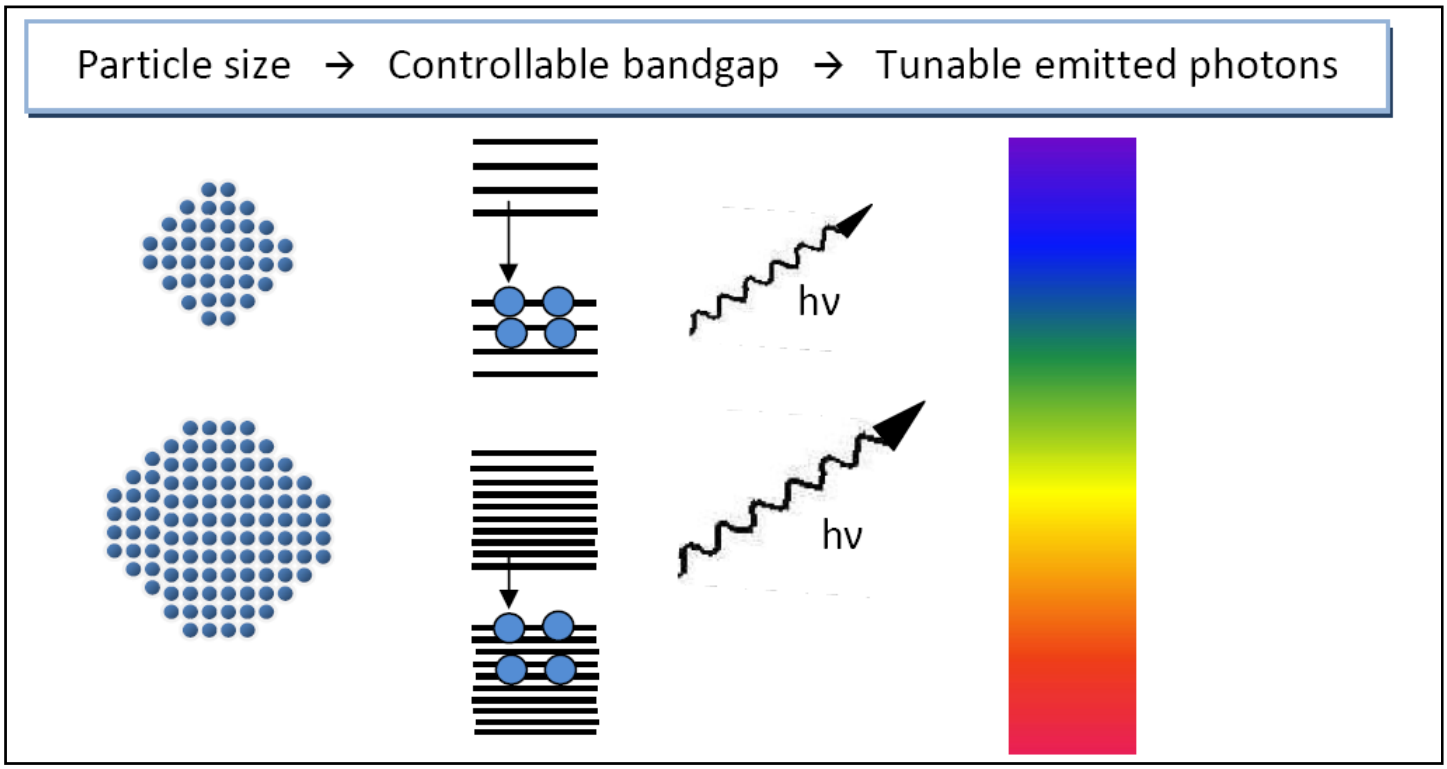

Figure 8 - Diagram showing the direct correlation of quantum dot size leading to different sized band gaps and different wavelengths of emitted photons.

1.2 Quantum Dot Synthesis

Quantum dot synthesis begins with the synthesis of two precursor solutions, one containing a selenium compound; the other containing dissolved cadmium ions. Mixed together at room temperature, there is no reaction; however, at higher temperatures an oxidation-reduction reaction occurs whereby crystals of cadmium selenide (CdSe) nucleate and grow [8]. Extraction of samples from the reaction vessel at different time intervals halts the reaction; thus allowing some control over the spectrum of particle sizes synthesized.

Cal Poly graduate Aaron Lichtner designed the process of synthesizing quantum dots at Cal Poly on the bulk scale (~15-20mL) [9]. In literature, similar processes have been developed on the micron scale by controlling the flow of the precursor solutions through microfluidic channels. These microfluidic reactors are placed over heat sources which allow the reaction to occur within the channels. Pump rate translates to residence time, which can be controlled to ensure tighter size distribution [10].

1.3 Microfluidic Reactor

A microfluidic reactor is a device that allows chemical reactions to occur in confined channels, with channel dimensions below 1 mm [11]. Microfluidic reactors are usually designed for continuous flow and offer many advantages over conventional scale reactions, including improvements in energy efficiency, reaction speed and yield, safety, reliability, scalability, on-site/on-demand production, and a much finer degree of process

control. Numerous microfabrication processes are necessary to create a microfluidic reactor, such as sputtering, photolithography, wet-etching, and reactive ion etching, to name a few.

1.3.1 Laminar Flow

Laminar flow occurs when two fluids flow together in parallel layers with no disruption between the layers. The equation that determines whether or not a system will experience laminar flow called the Reynolds Number [12],

$$R_e = \frac{\rho\, VD}{\mu_d}$$

where ρ is the density of the liquid, *V* is the velocity, *D* is the hydraulic diameter, and μ_d is the dynamic viscosity of the liquid. In the case where the channel shape is rectangular, then *D* is calculated as:

$$2ab / (a+b)$$

where a & b are sides of the rectangle. The Reynolds Number is a dimensionless number that gives a measure of the ratio of inertial forces to viscous forces. MEMS devices exhibit laminar flow if they have a Reynolds number less than 1000. The microfluidic reactor fabricated in this project has a Reynolds Number below 1, so laminar flow is exhibited and needed to be taken into account.

I ran tests that showed the bulk cadmium and selenium precursors can be mixed at room temperature and treated as a single solution. Testing of the CdSe solution showed that the system lacked sufficient heat for a rapid nucleation and growth reaction; thus,

as long as the solution was used the same day it was mixed, there was a negligible impact on the microfluidic nucleation and growth reaction.

It should be noted that after about a week, the original room temperature CdSe solution exhibited a significant broad spectral profile during fluorescence testing; therefore, while creating a single CdSe solution at room temperature was beneficial to avoiding mixing precursors through laminar flow, it was ideal that this solution was utilized for testing the same day it was created.

1.3.2 Fluid Resistance

Pressure builds quickly in a microfluidic device; therefore, it is essential to consider the variables that cause the device to fail due to pressure problems. One of the two major factors that play into pressure within the microfluidic reactor is fluid resistance. Fluid resistance is an indicator of the shear forces the walls of the channel exert on the liquid flowing through them, which for rectangular channels is calculated by:

$$R = \frac{12\mu_d L}{wh^3}$$

where μ_d is the dynamic viscosity of the liquid, L is the length of the channel, *w* is the width of the channel, and *h* is the etch depth of the channel [13]. In order to keep the pressure within failure limits; therefore, it is desirable to have a shorter channel length and a larger channel width and etch depth.

1.3.3 Volumetric Flow Rate

The other factor of pressure is the volumetric flow rate, which is a function of the syringe pump rate [13]. Volumetric flow rate (Q) is calculated by:

$$\mathbf{Q\ (m^3/s) = Pump\ Rate\ (m/s) * Cross\text{-}sectional\ area\ (m^2)}$$

The cross-sectional area is not a variable that can easily be altered between tests; however, the pump rate can be altered to adjust the volumetric flow rate.

1.3.4 Pressure Required to Drive the Fluid

The total pressure in the channels is calculated as the product of ***fluid resistance*** and ***volumetric flow rate*** [13]:

$$\Delta P_{\mu} = R * Q_{\text{flow rate}}$$

The pressure forces are necessary to balance the viscous forces due to the shear stresses on the channel walls. Once all factors are considered, variation in etch depth (*h*), pump rate (velocity), and length (L) allow for adjustments to be made to the pressure inside the microfluidic reactor.

1.3.5 Residence Time

Synthesizing quantum dots on the bulk scale can be characterized as controlling the temperature and the time allowed for the CdSe nucleation and growth reaction. In the microfluidic reactor, the time the fluid is running through the channels is called the residence time. A simple calculation between the velocity of the fluid and the distance

the fluid travels through the channel will give an approximate resident time; however, the channel volume is considerably smaller than the outlet tubing. As a result, the fluid is actually on the chip for a longer period of time than what is determined from the calculations.

1.4 Broader Impacts

There are a variety of fields that benefit from the use of quantum dots, such as photovoltaics, light-emitting diodes (LEDs), and biology. These three fields have the greatest demands for quantum dots and offer the most promising short-term benefits to society. Additionally, careful considerations must be made to identify the pros and cons of quantum dot synthesis in areas such as manufacturability, environmental impact, economic impact, sustainability, ethical considerations, health and safety.

1.4.1 Benefits to Science and Engineering

In the field of photovoltaics, quantum dots increase the efficiency and reduce the cost of the typical silicon photovoltaic cell. A layer of quantum dots applied to a solar panel can convert otherwise unused UV light from the sun into visible light that can make electricity [14]. Quantum dots made of lead selenide can produce as many as seven excitons from one high energy photon of sunlight (7.8 times the bandgap energy) [15]. Conversely, today's photovoltaic cells manage only one exciton per high-energy photon, with high kinetic energy carriers losing their energy as heat. Theoretically, solar cell efficiency could increase around 31% to 42%. An additional advantage with quantum

dot photovoltaics is that they are cheaper to manufacture, as they can be made using simple chemical reactions [16].

In recent years, there have been several promising inquiries into using quantum dots for LEDs to make displays and other solid state lighting sources. Quantum dots are valued for displays because they emit light that more accurately renders colors that can be perceived by the human eye. Additionally, quantum dots require very little power since they are not color filtered. Displays that intrinsically produce monochromatic light can be more efficient, since more of the light produced reaches the eye [17].

In modern biological analysis, a variety of organic dyes have typically been used. However, there has been increased demand in the flexibility of these dyes [18]. Quantum dots fill the role because they are superior to organic dyes on several counts. Quantum dots are considerably brighter (owing to a high extinction coefficient combined with a comparable quantum yield to fluorescent dyes [19]), as well as more stable. A typical use would be to attach antibodies or small-molecule ligands to target quantum dots that are specific to proteins on cells. One case study shows that researchers were able to observe quantum dots in the lymph nodes of mice for more than 4 months [20].

The purpose of this project is to create a method of synthesizing CdSe quantum dots with uniform sizes on a microscopic scale. Once achieved, the process could save the university significant money in the purchase of raw materials by eliminating waste. The financial stakeholders are the Materials Engineering Department at Cal Poly, or other

departments that desire a cheap, consistent fabrication process for quantum dots, such as BMED and CHEM Departments.

1.4.2 Manufacturability

The creation of quantum dots requires multiple steps, each one with precise control over variables. Recent research has shown that high quality, robust quantum dots can be created using bench-top techniques [8]. While it is important that these low-tech synthesis methods do not reduce the quality or reliability of the quantum dots produced, the focus of my senior project will be to develop a microfluidic process that can reduce the complexity and “guess work” of quantum dot production while still producing a high-quality reliable product.

1.4.3 Environmental Effects

The life cycle of quantum dots is related to the life cycle of the chemicals in their synthesis, which tend to be carcinogenic and environmentally harmful. Scientists today are focusing on what will happen when society begins to dispose of consumer products that contain quantum dots. Current research is investigating how quantum dots move through soil and water, and how the particles can accumulate in plants and earthworms. As quantum dots are mass produced in commercial products, the transport of quantum dots and metal oxide nanoparticles in the environment is a key concern [21].

1.4.4 Economic Factors

The complicated and specialized techniques required to make quantum dots are relatively expensive. A large majority of the cost comes from the solvents involved in making the quantum dot precursor solutions. These costs are the main barrier for those wishing to work with them, particularly at the university level. Commercially-made quantum dots range from $200 - $800 for 5mL of solution, which is not a cost many companies or research facilities can sustain [5]. Similarly, non-toxic phosphor dots go for $70 - $400 per mL [22].

The quantum dot project began at Cal Poly to create a viable method of producing quantum dots to be used for research in Cal Poly's Nanotechnology Lab [9]. Given the high cost of commercially produced quantum dots, a method for fabrication of the quantum dots at Cal Poly labs was developed; however, the current method is on a bulk scale. Synthesis on this scale; though, has not been shown to allow much user control on achieving desired quantum dot sizes. As a result, the user must use 'guess work' to create quantum dots and characterize them to ascertain the size developed, resulting in the repetition of the experiments that can increase costs and create waste.

My senior project is to design and manufacture a microfluidic reactor that synthesizes CdSe quantum dots under tightly controlled conditions. Precise control over pump rate and temperature should allow future users to achieve desired uniform quantum dot sizes every test run, which will limit waste from repeat experiments.

1.4.5 Sustainability

My senior project has designed a process for creating a reusable microfluidic reactor, such that future students can create the chip and use it repeatedly for synthesis of quantum dots. The main housing of the microfluidic reactor (silicon anodically bonded to Pyrex®) is a permanent fixture that can be used for repeatable and reproducible quantum dot synthesis. Minor components can be replaced every few syntheses, but the overall microfluidic reactor is sustainable and thus, a cost effective trade-off for synthesizing CdSe quantum dots.

1.4.6 Ethical Considerations

There are often unknown risks or unintended consequences to developing new technologies. The advantages to developing quantum dots are well known, but there is much that is still unknown about the risk to the human and natural environments. Consideration must be made to these areas of concern throughout all stages of development and disposal of quantum dots and their precursor solutions. My senior project follows all standard lab procedures dealing with the chemicals involved in microfabrication, as well as quantum dot synthesis and disposal.

1.4.7 Health and Safety Issues

In this project, the quantum dots are made from heavy metals and toxic chemicals, namely cadmium and selenium, which pose serious risks to the health of the people handling them, as well as the environment. There are restrictions worldwide on the use

of heavy metals in many household goods, which mean that most cadmium-based quantum dots are unusable for consumer-good applications [23].

ZnS coatings are being explored by other Cal Poly students in order to increase the intensity of the fluorescence of the quantum dots. The ZnS coating may react in water creating toxic hydrogen sulfide, in addition to being air and moisture sensitive [24].

One of the more serious issues with quantum dots is their potential in vivo toxicity when used in biomedical applications. CdSe nanoparticles are highly toxic to cultured cells under UV illumination. The energy of UV irradiation is close to that of the covalent chemical bond energy of CdSe nanoparticles. As a result, semiconductor particles can be dissolved, in a process known as photolysis, to release toxic cadmium ions into the culture medium. In the absence of UV irradiation, however, quantum dots with a stable polymer coating have been found to be essentially nontoxic [25]. However, little is known about the excretion process of quantum dots from living organisms, so careful examination must be made before quantum dot applications in tumor or vascular imaging can be approved for human clinical use. [26]

2 Methods and Materials

2.0 Process Design

The fabrication of the microfluidic reactor was due to a variety of microfabrication steps. A silicon wafer was used as the bottom substrate of the reactor and was processed by aluminum sputtering, photolithography, wet chemical reactions and reactive ion etching. Pyrex® was used for the top substrate and the only preparation needed was to drill holes through the glass. An anodic bonding process was used to bond the two substrates together. The bulk CdSe solution was interfaced from a single syringe into the microfluidic reactor by using Tygoprene® and stainless steel tubing and plasma bonding PDMS. Synthesizing QDs was possible by controlling the pump rate with a syringe pump and placing the microfluidic reactor on a hot plate set at 225^{o}C. The synthesized QDs flowed out of reactor and were collected in a small vial for analysis. Finally, the QDs were characterized by exposing them to an excitation source (blue LED) and measuring the fluorescence spectral profile.

2.1 Process Development

A Syringe Pump® Model NE-300 syringe pump was used to ensure pump rate remained constant in each test. The syringe pump allowed for a variety of syringe types to be used and the pump rate was based on the inner diameter of the syringe. The goal of this project was only to create a microfluidic reactor that allows for synthesis of CdSe QDs to occur; therefore, a Design of Experiment (DOE) was not a primary objective.

However, a full DOE may include a range of different pump rates, etch depths, temperatures, or channel lengths.

Since bulk QD synthesis involved mixing the two precursor solutions at 225^{o} C, that temperature was determined to be the ideal temperature to set the hot plate. The temperature within the channel was probably lower than this temperature, but the microfluidic reactor was not designed to accommodate a thermocouple. Regardless, CdSe QDs have been shown to nucleate and grow at temperatures as low as 180^{o}C; therefore, 225^{o}C on the hot plate was sufficient enough to synthesize QDs in the microfluidic reactor.

2.1.1 Lab Setup

Synthesis of cadmium and selenium precursors took place in a fume hood due to the toxic nature of the two chemicals. Also, since octadecane makes up the majority of the CdSe solution, it was best to carry out the microfluidic reaction procedure under a fume hood because octadecane fumes can irritate exposed eyes.

The following pieces of lab equipment were used to create and operate the microfluidic reactor:

Clean Air Products fume hoods (Model CAP1411-636-36H-PPHB & SSHB)

Torr CrC-150 Sputtering System with DCG-200 DC Plasma Generator

Laurell Spin Coater (Model WS-400B-6NPP/LITE/AS)

Canon Parallel Light Mask Aligner (Model PLA-501FA) with Ushio Mercury Lamp Power Supply (Model HB-25105AP)

Semitool Spin/Rinse/Dryer (Model PSC-101)

AGS RIE System (Model 1700-RIE) with ACG-6B RF Generator and Fluke 73III multimeter

TriStar Technologies Duradyne Plasma Surface Treatment Station (Model PT-200P)

Ambios Technology Profilometer (Model XP-1)

Hitachi 10" Bench Drill Press (Model B13F)

Quincy Lab Oven (Model 10)

Ocean Optics Spectrometer (Model USB4000)

GW Laboratory DC Power Supply (Model GPR-30H10D)

Torrey Pines Scientific Hot Plate/Stirrer (Model HS50)

Torrey Pines Scientific Hot Plate (Model H50)

Barnstead|Thermolyne CIMAREC Hot Plate

Thermoscientific CIMAREC Hot Plate

Syringe Pump (Model NE-300)

2.1.2 Reaction Procedure

Under ideal conditions, the CdSe solution reacts by a nucleation and growth reaction. CdSe clusters will grow as long as they are allowed to react. The microfluidic reactor was the environment for this chemical reaction to take place. The reactor temperature was controlled by setting on a hot plate at 225^{o}C. The pump rate of syringe pumps

ensured the reaction took place while moving through the microfluidic reactor channels and ended when the QDs came through the outlet of the device.

2.2 Microfabrication Processing Methods

2.2.1 Sputtering Aluminum

The first step to creating the microfluidic reactor was to secure a p-type silicon wafer with a <1-0-0> crystallographic orientation. Aluminum was needed as a mask for creation of the microfluidic channels by protecting areas of the silicon wafer that did not need etching. Following the Standard Operating Procedure (SOP) for the Torr CRC-150 Sputtering System, an even layer of aluminum was sputtered over the surface of the silicon wafer (Figure 9) using the parameters shown in Table I.

Figure 9 - Cross section of silicon wafer with a layer of aluminum deposited on top

Table I - Parameters for Sputtering Aluminum on Silicon Wafer

Pressure, mTorr	Power, Watts	Pre-Sputter time, min	Sputter time, min	Sputter rate, Å/ min
0.015	60	2	15	750

Argon ions bombarded an aluminum target, knocking off aluminum atoms. The resultant aluminum vapor deposited aluminum atoms on the silicon substrate (Figure 10).

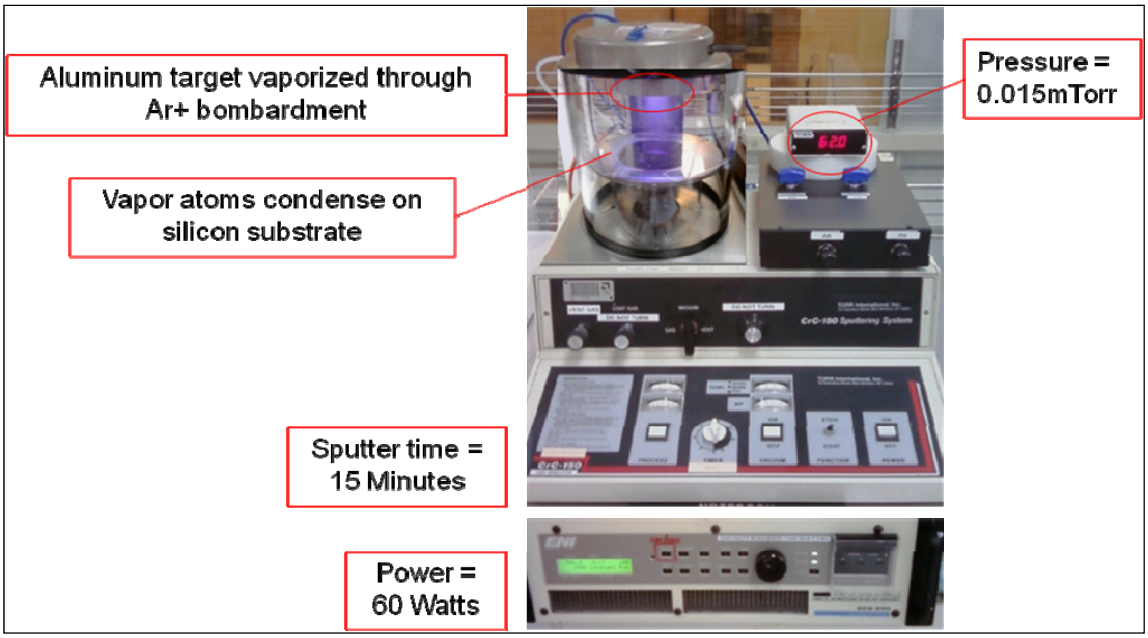

Figure 10 - The CRC-150 Sputtering System created an aluminum vapor fog that deposited aluminum atoms in an even layer on the silicon substrate.

2.2.2 Photolithography

The next step was to use photolithography to get the image of the channels onto the aluminum mask. The SOP was followed for using the Laurell Spin Coater (Figure 11).

Figure 11 - The Laurell Spin Coater was used to evenly apply a layer of positive photoresist on top of the aluminum mask layer

Once loaded in the vacuum chamber, spin-coating began by dispensing MicroChem Primer 80/20 [containing 80% Hexamethyldisilazane (HDMS)] (~3mL) onto the wafer. During the spin coat process, 3-4mL of positive resist (Shipley 1813) was dispensed on the wafer (Table II).

Table II - Process Parameters for Spin Coating

Step	Purpose	Time, Sec	Spin speed, RPM
1	Post-Dispense HMDS	30	300
2	Spread HMDS	20	3000
Pause cycle and dispense 3-4mL of Positive Resist			
3	Spread Resist	20	200
4	Spread Resist	10	500
5	Planarize Resist	20	4000
6	Slow & Stop	5	300

To ensure complete resist coverage, the entire spin-coating process was repeated a second time, excluding the dispensing of HMDS. This was necessary because a single coating often times yielded spots in the positive resist due to lab contamination. A second coating covered those spots with positive resist. Upon completion of the spin coating cycle, the wafer was soft baked at 90^{o}C for 60 seconds to drive off solvents, followed by 10 seconds on a cold plate to chill.

Next, the wafer was run through the photolithography aligner for exposure to UV light following the SOP (Figure 12; Figure 13).

Figure 12 - The Photolithography Aligner allows the user to expose their device to UV light through a mask layer which has a desired pattern

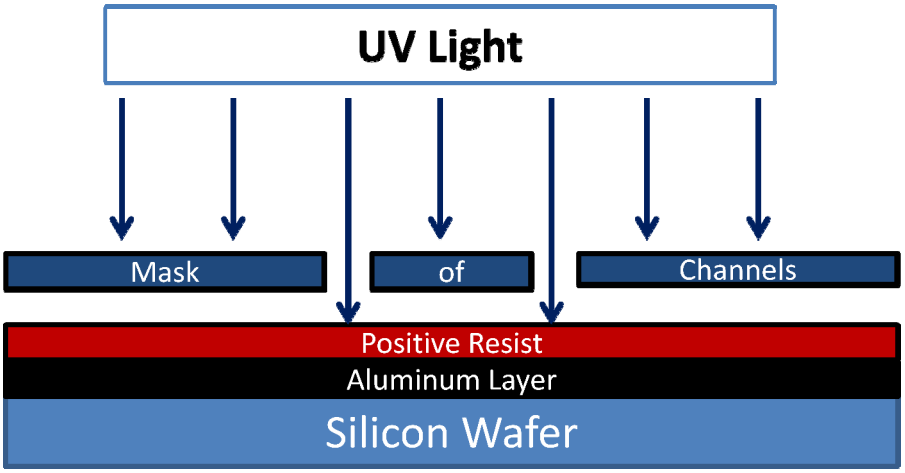

Figure 13 - Cross section showing that the positive photoresist will only be exposed to UV light in areas where the mask is has openings

The mask used was a modification of a mask that had one long continuous channel.

Using black electrical tape, modified channels of 2.5, 5.0, and 7.5cm were created

(Figure 14).

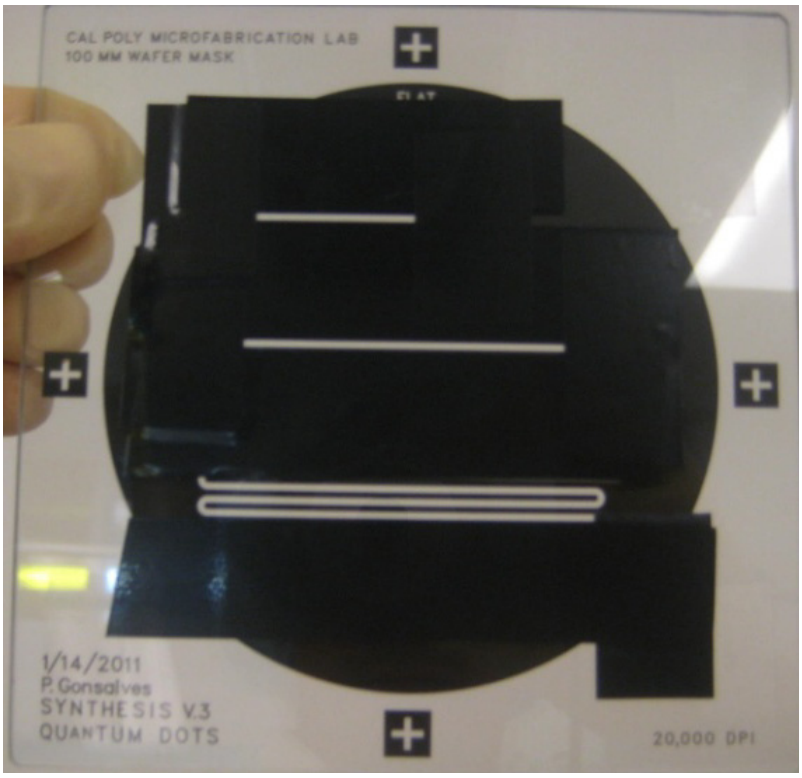

Figure 14 - The mask was designed to only allow light to expose specific areas of the wafer, namely 2.5, 5, and 7.5cm channels.

The parameters for running the photolithography aligner are shown in Table III.

Table III - Process Parameters for Photo Alignment

Dose, mW/cm^2	Alignment Gap, µm	Print Gap, µm	Light Integral	Exposure Time, sec
6.5	30	10	4.0	14.85

Immediately after exposure, the wafer was developed in Microposit CD-26 Developer [2.5% Tetramethylammonium hydroxide (TMAH)] using the parameters in Table IV.

Table IV - Process Parameters for Developing Exposed Positive Photoresist

Time, minutes	Temperature, ^{o}C	Agitation? (Y/N)
2	Room Temp	Yes

Finally, the wafer was hard baked at 150°C for 60 seconds, followed by 15 seconds on a cold plate to chill (Figure 15).

Figure 15 - Cross section showing that the developing solution will etch the channel design into the positive resist in areas that were exposed to UV light.

2.2.3 Wet Etching and Resist Strip

The next step was to etch the channels into the now-exposed aluminum mask (Figure 16).

Figure 16 - Cross section showing that aluminum etchant will etch the channels into the areas of aluminum that were exposed to the etchant

This was done using an aluminum etchant [Acetic acid, Nitric acid, Phosphoric acids; Transene: Type A]. The etch parameters are shown in Table V and were conducted on a hot plate under a fume hood. The temperature was monitored with a thermometer.

Table V - Process Parameters for Aluminum Etching

Time, minutes	Temperature, °C	Etch Rate, Å/sec	Agitation? (Y/N)
2	50	750	Yes

Once the channels were etched down to the silicon wafer, Microposit Remover 1165 [94-95% 1-methyl-2-pyrrolidinone; 5-6% Pyrrolidone Compound] was used to strip off the remaining positive resist (Figure 17).

Figure 17 - Cross section showing the silicon wafer with an aluminum mask layer protecting areas that were not to be etched.

The parameters for stripping off the positive resist are shown in Table VI and were also conducted on a hot plate under a fume hood. The temperature was again monitored using a thermometer.

Table VI - Process Parameters for Stripping Positive Resist

Time, minutes	Temperature, ^{o}C	Agitation? (Y/N)
15	70	Yes

2.2.4 Reactive Ion Etching

Reactive Ion Etching (RIE) was carried out on the wafer following the SOP (Table VII).

Table VII - Process Parameters for Reactive Ion Etching

Ratio, SF_6:O_2	Base Pressure, mTorr	Power, Watts	Etch Time, minutes	Etch depth, μm
80:20	300	300	40	40

The RIE process was an anisotropic dry etching process that etched the microfluidic channels into the silicon wafer. During RIE, the wafer sat on an electrode which created a negative bias that accelerated positively charged ions toward the substrate (Figure 18).

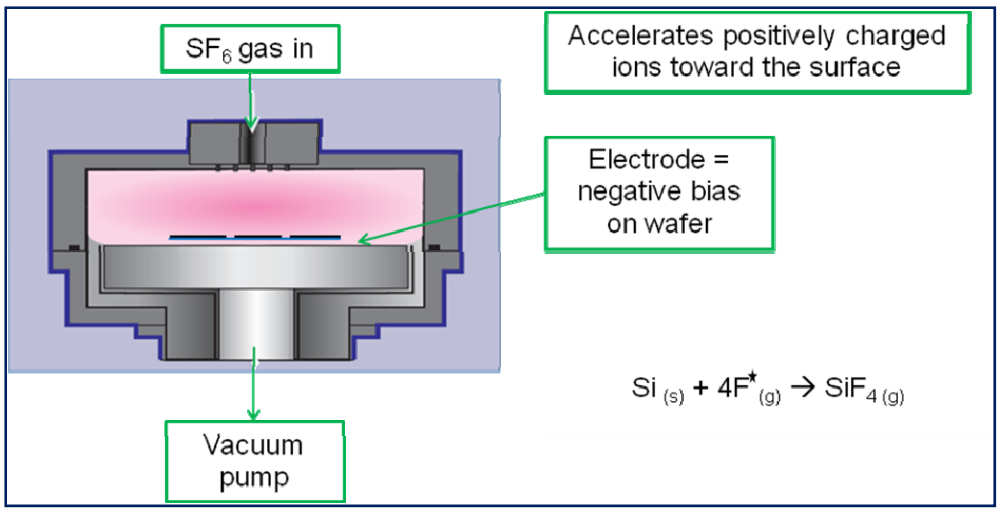

Figure 18 - Reactive Ion Etching is an anisotropic dry-etching process whereby fluorine radicals aggressively react with the exposed silicon wafer

RIE is a highly selective process; reacting with the silicon much more aggressively than the aluminum. Since fluorine radicals are highly reactive with silicon, the etching took place at approximately 1 μm/min. The resultant volatile SiF_4 gas was evacuated from the chamber into the atmosphere; thus, the channels were etched into the silicon (Figure 19).

Figure 19 - Cross section showing the etched channels that result from Reactive Ion Etching

Once the desired etch depth was achieved, the aluminum mask was stripped off using the aluminum etchant and the process parameters in Table V. The result was a complete silicon substrate ready for anodic bonding (Figure 20).

Figure 20 - Cross section showing etched silicon wafer after stripping off the aluminum mask

2.2.5 Drilling Holes in Pyrex®

For a glass substrate, Pyrex® was chosen specifically based on composition (Table VIII) and thermal coefficient of expansion. The intermetallic compounds present were necessary in order for anodic bonding to be possible in the next step. Also, since anodic bonding involves high temperature, it was important to choose a glass material that has a similar thermal coefficient of expansion as the silicon wafer to avoid the glass shattering during anodic bonding.

Table VIII - Composition of Pyrex® Borosilicate

Compound	% Composition
SiO_2	81
B_2O_3	13
Na_2O	4
Al_2O_3	2

The Pyrex® wafer was aligned over the original mask to identify the location of where the inlet and outlet holes were to be drilled (Figure 21).

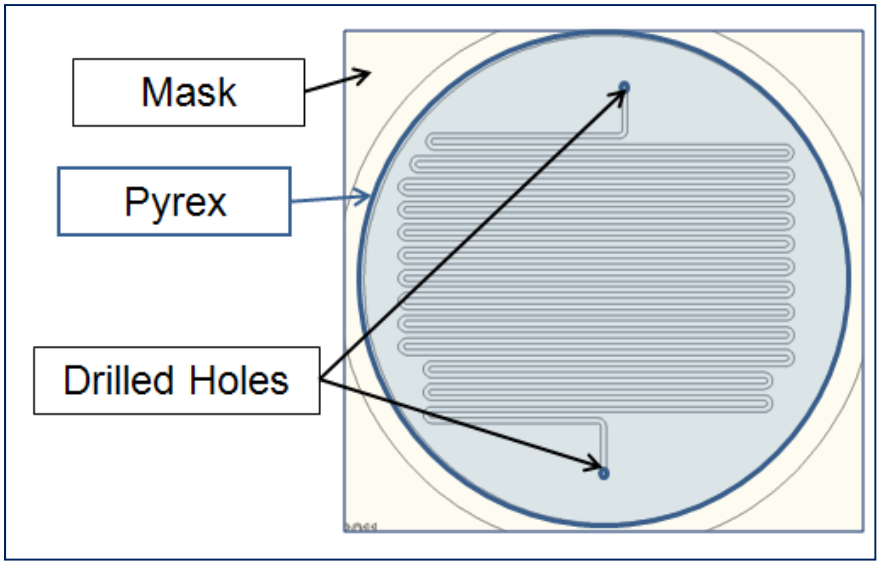

Figure 21 - The Pyrex® wafer is lined up over the mask layer and marked to identify where the inlet and outlet holes will go

Drilling through glass created small chips around the “breakthrough” side of the hole. These chips could have caused problems during the anodic bonding step that occurred next. Since the chipping was virtually non-existent on the side of the glass wafer that drill bit contact was initiated, it was imperative that the holes were drilled from the “anodic bonding side” (Figure 22).

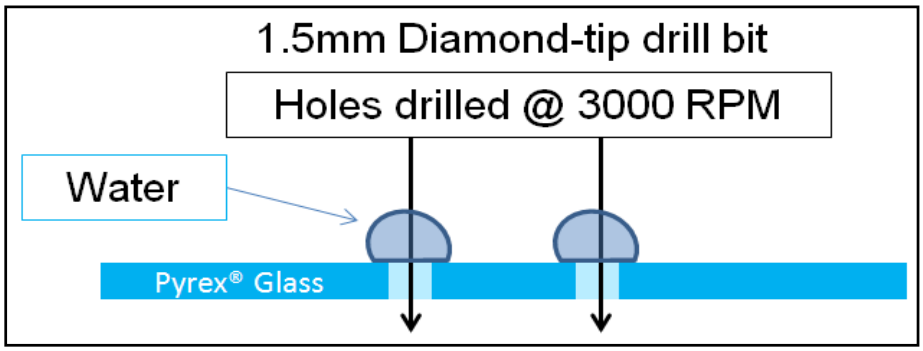

Figure 22 - Cross section showing how holes can be drilled through a Pyrex® wafer with minimal chipping around the edges

2.2.6 Anodic Bonding

The main reason that Pyrex® glass was chosen as the top substrate for the microfluidic reactor was due to composition. Ions were necessary in order to be able to create an anodic bond with the silicon wafer. An aluminum block was placed on a hot plate, followed by the silicon wafer. The Pyrex® wafer was set on top of the silicon wafer with care to make sure that the drilled holes lined up with the etched inlet and outlet holes on the silicon wafer. Finally, another aluminum block was placed on top of the Pyrex® wafer (Figure 23).

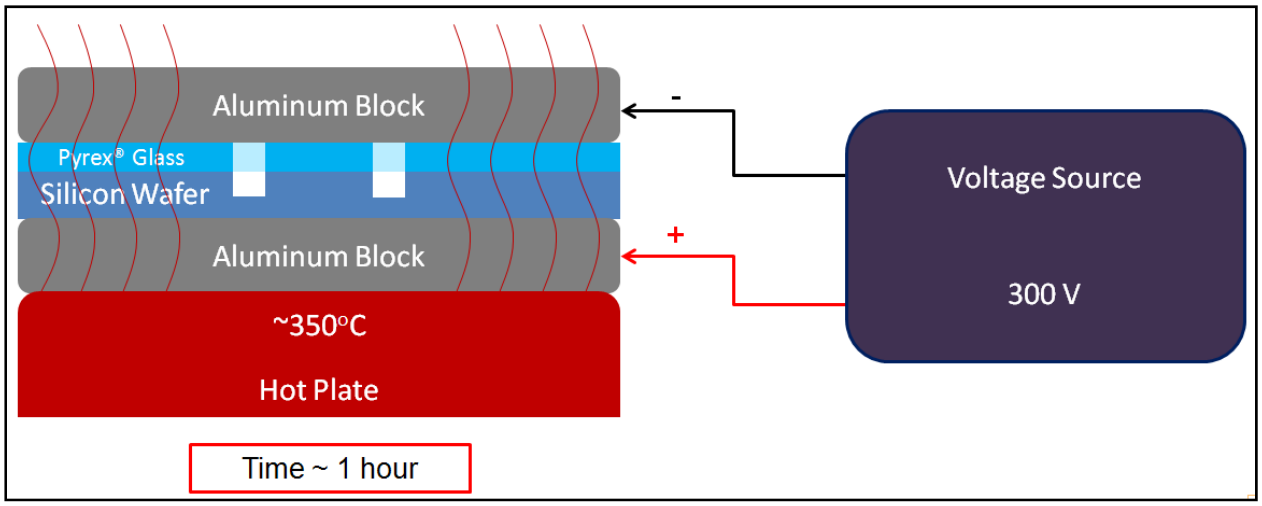

Figure 23 - Cross section showing the anodic bonding testing apparatus. The hot plate allowed for ion diffusion in the solid substrates, while the voltage was the driving force for anodic bonding to occur.

A negative charge was attached to the top aluminum block to attract Na^+ ions in the Pyrex® wafer. Conversely, a positive charge was attached to the bottom block which attracted electrons in the silicon. The process created an area at the interface between the silicon and Pyrex® where anodic bonding took place between the remaining O_2^- and Si^+ ions. The temperature increased the diffusion rate, while the voltage was the driving force for the reaction (Table IX). After approximately 1 hour elapsed, complete anodic bonding occurred between the silicon and Pyrex®.

Table IX - Process Parameters for Anodic Bonding

Temperature, ^{o}C	Pre-heat time, minutes	Voltage, V	Time, minutes
380	10	300	60

2.2.7 Interfacing Syringes to Microfluidic Reactors

The next challenge in creating the microfluidic reactor was to interface the bulk CdSe solution from a syringe to the microfluidic channels. Interfacing was possible by using Polydimethylsiloxane (PDMS) and a Duradyne Argon Plasma Surface Treatment Station (Figure 24, Figure 25).

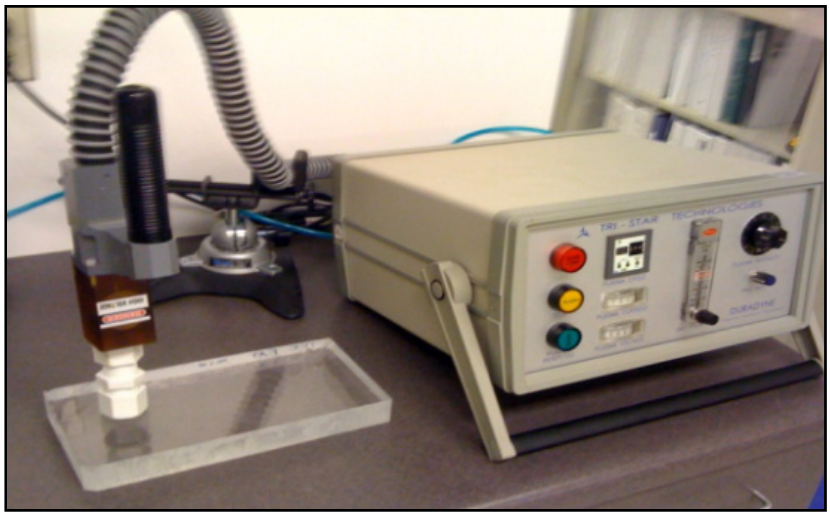

Figure 24 – Duradyne argon plasma system

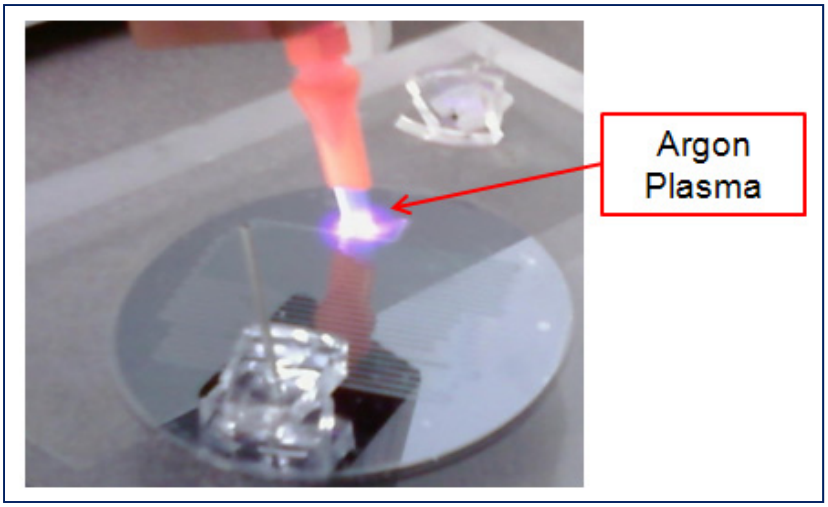

Figure 25 - Close-up of Argon plasma being applied to the surface of the Pyrex® wafer for the purposes bonding to PDMS

PDMS was created in a 3-inch plastic Petri dish following the SOP. The cured PDMS was cut into small 1 inch by 1 inch cubes. These PDMS cubes were "punched" with 16 gauge stainless steel (SS316) needles. The needles remained in the PDMS and Tygoprene® tubing was affixed over the end of the SS316 that led back to the CdSe syringe (Figure 26) on one side and to a vial for collection on the other.

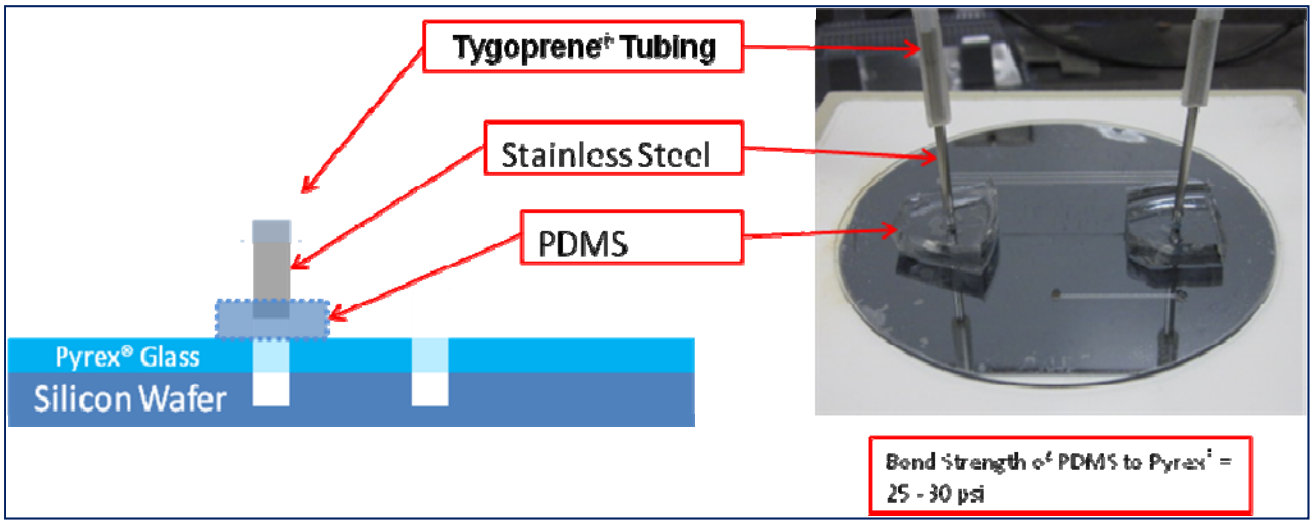

Figure 26 - Cross section of PDMS and microfluidic reactor showing interface material setup

2.2.8 Testing Setup

A syringe pump controlled the pump rate of the syringe that held the CdSe room temperature solution. The syringe was connected to Tygoprene® tubing that led down into the microfluidic reactor, which was set on a hot plate set at 225°C. Outlet tubing continued the flow of the solution back out of the microfluidic reactor and into a vial for storage until characterization (Figure 27; Figure 28).

Figure 27 - Testing involved using a syringe pump to control the pump rate (Volumetric Flow Rate), a hot plate to control the temperature, and a small vial to capture CdSe quantum dots out of the outlet tubing.

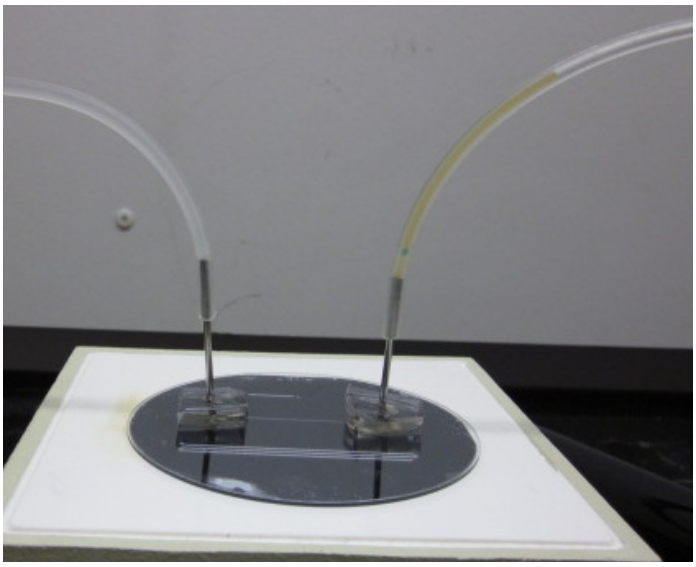

Figure 28 - Close-up of microfluidic device on the hotplate: the left tube contained a clear room temperature CdSe solution, while the right tube shows some color that indicated a chemical reaction had occurred on the hot plate.

In order to visualize during testing that CdSe QD synthesis had occurred, a black light was setup under the fume hood to observe fluorescence (Figure 29).

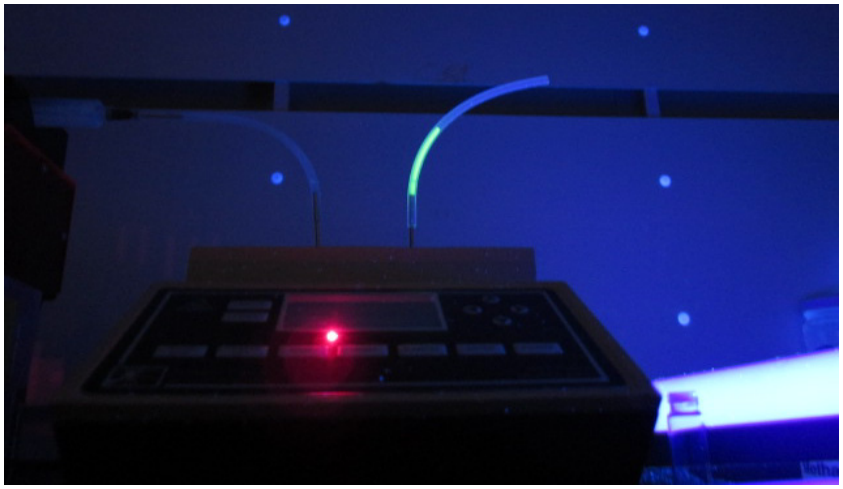

Figure 29 - Exposing the testing apparatus to a black light revealed that CdSe QDs were synthesized because of the fluorescence of the solution in the outlet tubing.

2.3 Characterization of Synthesized Quantum Dots

Quantum dots have the unique material property of fluorescing when exposed to an excitation source. The color of the light fluoresced is an indicator of the size of the quantum dot; thus, fluorescence testing was used to confirm that QD synthesis had occurred within the channels of the microfluidic reactor.

2.3.1 Fluorescence Testing

Fluorescence was the main characterization technique used in determining the size of quantum dots. Blue colors indicate CdSe QDs were around 2 nm in size, while dark red quantum dots would be approximately 5 nm. In order to test a QD sample, a small portion was placed in a quartz cuvette and the cuvette was exposed to an excitation light source. The resulting fluorescence was measured using an Ocean Optics USB4000 Spectrometer and software (Figure 30).

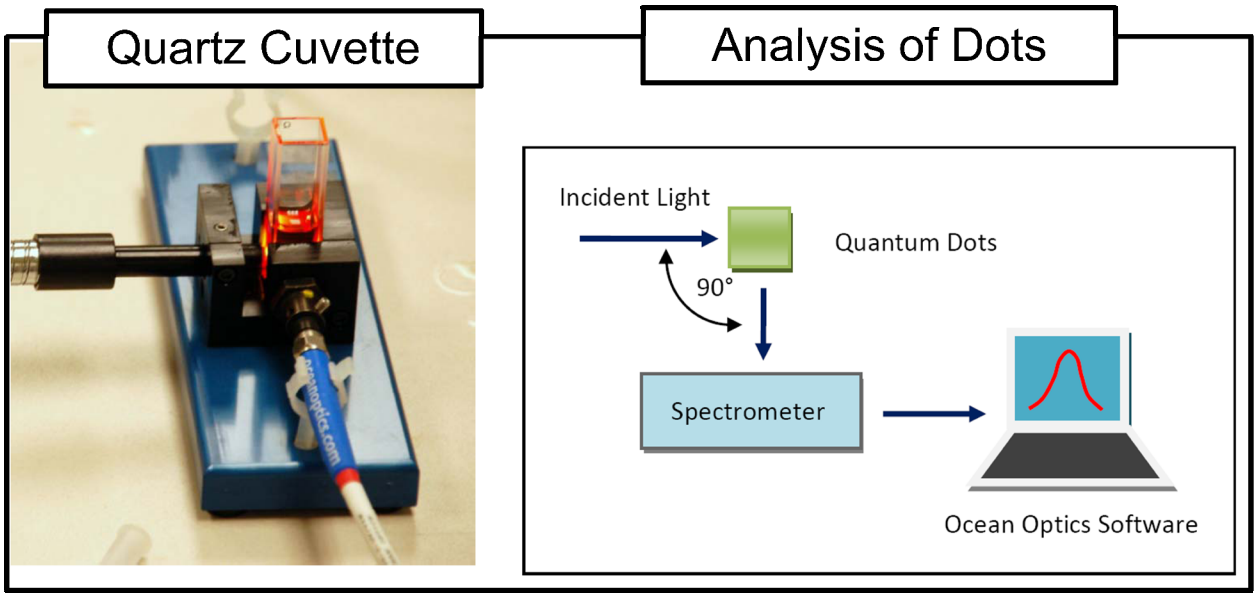

Figure 30 - Testing quantum dots for fluorescence involves putting a sample in a cuvette, exposing it to an excitation source (such as a blue LED), and measuring the resulting fluorescence with a spectrometer

3 Results

3.0 Spectrum and Repeatability

The spectrometer creates a graph depicting wavelength vs. intensity (Figure 31). A general trend found during testing was that the faster the pump rate, the shorter the residence time; therefore, the smaller the resultant quantum dots.

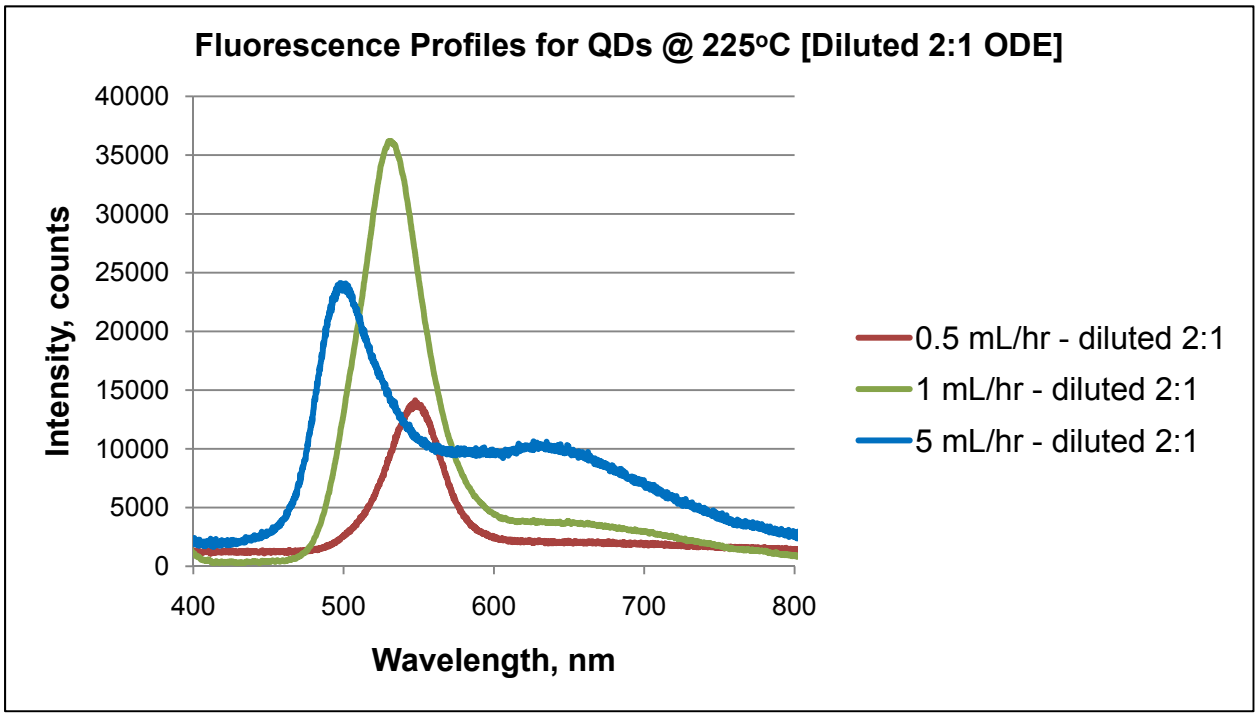

Figure 31 - Spectral profiles of three different successful syntheses showing the trend that faster pumping rates yield smaller quantum dots

3.1 Full-Width-Half-Maximum

The ideal spectral profile would be a vertical line at a given wavelength indicating that the entire synthesis of quantum dots were the same size; however, a typical quantum dot synthesis is not an ideal reaction. The best method for characterizing fluorescence is by a method called the full-width-half-maximum (FWHM). To measure the FWHM, we must first identify the peak intensity value (counts), then calculate half this peak

intensity value. Once determined, subtracting the two wavelength values that intersect the half-maximum will result in the FWHM.

A long-term objective of microfluidic CdSe QD synthesis would be to reduce the FWHM as small as possible. At the very least, it is desirable to achieve similar FWHM values that are made through the bulk synthesis method; however, improving on these numbers should be an advantage of using the microfluidic reactor.

3.2 Pressure

One of the largest obstacles to an operational microfluidic reactor was to ensure the variables kept the pressure in the reactor below the bursting strength of the PDMS-Pyrex® bond. The bond strength of PDMS to Pyrex® has been shown to be around 25 psi [27]. Using pressure calculations, the pressure is shown to be well below this burst strength (Table X).

Table X – Relationship between Pump Rate, Pressure and Residence Time

Pump Rate, mL/hr	Pressure, kPa	Pressure, psi	Residence Time in Channel, sec	Residence Time on device, sec
0.5	1.737	0.252	15	~40
1	3.474	0.504	8	~20
5	17.368	2.520	4	~10

Bond Strength of PDMS to Pyrex® = 25 - 30 psi

Estimated

4 Discussion

4.0 Macroscopic vs. Microscopic

The bulk synthesis method in the Cal Poly Nanotechnology Lab has been shown to achieve fluorescence values of 480nm (blue-green) up to about 600nm (red). The objective of my project was to only to synthesize CdSe QDs through the microfluidic reactor, which was achieved; however, a more desirable goal would be to synthesize QDs that fluorescence below 480nm (blue) or above 600nm (red), in addition to creating a narrower full-width-half-maximum.

4.0.1 Can the Microfluidic Reactor Synthesize Blue or Red Light?

Faster pump rates have been shown to synthesize smaller QDs in the microfluidic reactor; however, there is also a corresponding increase in pressure. Testing should reveal the actual threshold pump rate that will minimize the residence time of the nucleation and growth reaction. It may be possible to experimentally achieve a blue fluorescence; however, it will be difficult to stop the reaction quickly enough to stop growth once out of the channel. Implementing a heat sink on the outlet tubing may assist in “quenching” the reaction.

Conversely, it appears that slower pump rates will carry the growth reaction long enough to yield larger QDs (around 600nm); therefore, it should be possible to pump the CdSe solution through the microfluidic reactor slow enough to allow a similar result. An advantage of using a microfluidic reactor to synthesize CdSe QDs is the ability to

better control the reaction environment and theoretically achieve more discrete FWHM spectral profiles, in addition to wavelengths that are not achievable on the bulk synthesis scale.

4.0.2 The Tail for High Residence Times

Faster pump rates yield CdSe QDs of smaller sizes; however, there exists a broad tail in the high wavelength region of the graph (Figure 31). The tail occurs because as some QDs go through nucleation and growth, another wave of QDs is also going through nucleation and growth, followed by a different group of QDs, and so on. The result is a series of larger QDs that will fluorescence at a lower intensity than the initial peak that dominates the solution. Removing the tail may be possible by inserting a heat sink on the microfluidic reactor to halt the growth reaction of the QDs as they come out of the microfluidic channels.

4.0.3 Dilution Effects

The relative intensity of fluorescence is around 5000 counts when the CdSe QDs are synthesized through the microfluidic reactor. The intensity can be increased as much as 10 times when diluted with additional octadecane. A 2:1 ratio of octadecane to CdSe QD solution appears to be ideal. The reason dilution increases the intensity is simply because by diluting the QDs, more light can be fluoresced.

5 Conclusions

The successes and failures of the project are numerous:

1. Cadmium selenide can be mixed at room temperature and treated as a single solution for injection into a microfluidic reactor if it used the same day the solution is synthesized.
2. Anodic bonding of silicon and glass substrates is possible as a means to create a microfluidic reactor.
3. PDMS can be used successfully to interface a bulk solution to the microfluidic channels of a microfluidic reactor.
4. Pressure can be kept under control by keeping channel length short and pump rate low.
5. Fluorescence spectral profiles reveal that the full-width-half-maximum is as wide as bulk synthesis fluorescence profiles, indicating the need to install a heat sink on the microfluidic reactor to halt the nucleation and growth reaction sooner.

6 Future Work and Recommendations

- Create a DOE comparing etch depth, pump rate, channel length and temperature, in order to determine the best method for achieving the narrowest full-width-half-maximum.
- Design a heat sink on the microfluidic reactor to ensure the CdSe QD reaction will cease.
- Design the microfluidic reactor to accommodate thermocouples to identify the actual temperature of the nucleation and growth reaction.
- A mask design with channels that have a smaller width than the 1000 microns used in this project may be more ideal to control the reaction conditions; however, a shallower etch depth may also compensate for such a wide width.

7 References

[1] Schmid, G., ed. Nanoparticles: From Theory to Application. New York: John Wiley & Sons, Incorporated, 2004.

[2] Magee, Greg. “Nanomedicine.” http://chem3513-2007.pbworks.com/w/page/15648426/Nanomedicine

[3] Grandinetti Laboratory. Chem 121 – General Chem Lectures. April 3, 2011. http://www.grandinetti.org/Teaching/Chem121/Lectures/MOTheory/?vm=r

[4] Zumdahl, Steven S. Zumdahl, Chemistry Principles With Cd, 4th Edition Plus Chemistry, Chemical Office Limited, 1st Edition. Boston: Houghton Mifflin Company, 2001

[5] Evident Technologies. "How Quantum Dots Work." www.evidenttech.com.07 October 2010 http://www.evidenttech.com/quantum-dots-explained/how-quantum-dots-work.html

[6] Blaylock, Guy. Introduction to Modern Physics. UMass. May 1999. http://www-unix.oit.umass.edu/~blaylock/p284/

[7] Salisbury, David F. "Quantum dots that produce white light could be the light bulb's successor." Exploration - Vanderbilt University (2005).

[8] Pradeep, T. Nano. New York: McGraw-Hill Professional, 2008.

[9] Lichtner, Aaron. “Process Development and Characterization of Cadmium Selenide Quantum Dots Synthesis through Nanoparticle Size Optimization.” Cal Poly Senior Project. 5 June 2009

[10] Uehara, Masato, et al. “Synthesis of CdSe/ZnS/ZnS Quantum Dot Quantum Well in a Micro Reactor.” IFMBE Proceedings. Volume 14/1.

[11] Recent advances in synthetic micro reaction technology Paul Watts and Charlotte Wiles Chem. Commun., 2007, 443 - 467

[12] Benson, Tom. “Reynolds Number”. National Aeronautics and Space Administration. May, 2009. http://www.grc.nasa.gov/WWW/BGH/reynolds.html

[13] Bhushan, Bharat, Editor. *Springer Handbook of Nanotechnology*. 2nd edition. New York. 2007

[14] Savage, Richard, Hans Mayer, Matthew Lewis, and Dan Marrujo. "Utilizing Quantum Dots to Enhance Solar Spectrum Conversion Efficiencies for Photovoltaics." Materials Research Society (2008).

[15] Service, Rf. "Materials Research Society fall meeting. Shortfalls in electron production dim hopes for MEG solar cells." *Science.* Vol. 322. No. 5909. Dec 2008. pp. 1784.

[16] Talbot, Davis. *TR10: Nanocharging Solar*. Technology Review. March 12, 2007

[17] http://www.vanderbilt.edu/exploration/stories/quantumdotled.html. Exploration, Vanderbilt's Online Research Magazine - Shrinking quantum dots to produce white light

[18] Walling, M. "Quantum Dots for Live Cell and In Vivo Imaging". International Journal of Molecular Science. Vol. 10. No. 2, pp.441–491.

[19] X. Michalet, "Quantum Dots for Live Cells, in Vivo Imaging, and Diagnostics." Science Vol. 307. No. 5709, pp. 538 – 544

[20] Ballou, B. "Noninvasive imaging of quantum dots in mice." Bioconjugate chemistry. Jan 2004. pp. 79–86.

[21] Nanowerk News. "New instruments at UBuffalo will help scientists map tumor surfaces, study environmental impact of quantum dots." Feb 10, 2011. http://www.nanowerk.com/news/newsid=20097.php?vm=r

[22] Sun Innovations, Inc. "Online Ordering." www.nanomaterialstore.com. 07 October 2010 http://www.nanomaterialstore.com/nano-phosphor.php

[23] Nanoco Group, PLC. "Cadmium-free quantum dots." www.nanocotechnologies.com. 08 October 2010 http://www.nanocotechnologies.com/content/AdvancedMaterials/CadmiumFreeQuantumDotsQFQDHeavyMetalFree.aspx.

[24] Evident Technologies. "CdSe/ZnS Core Shell Evidots in Toluene." www.evidenttech.com. 08 October 2010 http://msds.chem.ox.ac.uk/ZI/zinc_sulfide.html

[25] Pelley J. "State of academic knowledge on toxicity and biological fate of quantum dots". *Toxicological Sciences: an Official Journal of the Society of Toxicology*. 276–96

[26] Choi HS, Liu W, Misra P, Tanaka E, Zimmer JP, Itty Ipe B, Bawendi MG, Frangioni JV. Nature Biotechnology. Sept 2007. 1165-70. "Renal clearance of quantum dots".

[27] Bhattacharya, Shantanu. "Plasma Bonding of Poly(dimethyl)siloxane and Glass Surfaces and its Application to Microfluidics" Thesis. Texas Tech University. December, 2003.